

MICHAŁ LUPA<sup>1</sup>, KATARZYNA ADAMEK<sup>2</sup>, ANDRZEJ LEŚNIAK<sup>3</sup>, JAROSLAV PRŠEK<sup>4</sup>

## Application of satellite remote sensing methods in mineral prospecting in Kosovo, area of Selac

### Introduction

Satellite remote sensing techniques have been used for environmental research for over 45 years. Moreover, geological remote sensing has become a separate scientific subdivision that has found its application in many research problems. The information that can be obtained with the use of remote sensing techniques varies according to the sensors. The most commonly used remote sensing techniques are: airborne laser scanning, multispectral and hyperspectral optical scanners (Cloutis 1996; Fraser et al. 1997; Bedini et al. 2009; Zagajewski et al. 2017), the family of the SAR methods (Porzycka et al. 2014) and radar data (Joyce et al. 2014). Depending on the type of data, we are able to create a digital terrain model, classify land cover, recognize lineaments (Dasgupta and Mukherjee 2019) or identify minerals

✉ Corresponding Author: Katarzyna Adamek; e-mail: kadamek@agh.edu.pl

<sup>1</sup> AGH University of Science and Technology, Kraków, Poland; ORCID iD: 0000-0002-4870-0298; e-mail: mlupa@agh.edu.pl

<sup>2</sup> AGH University of Science and Technology, Kraków, Poland; ORCID iD: 0000-0003-2595-9296; e-mail: kadamek@agh.edu.pl

<sup>3</sup> AGH University of Science and Technology, Kraków, Poland; ORCID iD: 0000-0002-9442-0799; e-mail: lesniak@agh.edu.pl

<sup>4</sup> AGH University of Science and Technology, Kraków, Poland; ORCID iD: 0000-0003-4331-8273; e-mail: prsek@yahoo.com



© 2020. The Author(s). This is an open-access article distributed under the terms of the Creative Commons Attribution-ShareAlike International License (CC BY-SA 4.0, <http://creativecommons.org/licenses/by-sa/4.0/>), which permits use, distribution, and reproduction in any medium, provided that the Article is properly cited.

in geological outcrops. In the context of mineral prospecting, a significant development was the rise of imaging spectroscopy (Goetz et al. 1985). This method is based on optical sensors that are capable of acquiring images in many spectrally narrow bands. After the images have been acquired, remotely captured laboratory-like spectra can be distinguished and compared to those obtained in a laboratory. Today, this is an efficient method of exploring and mapping surface mineralogy by means of advanced algorithms and processes (Mierczyk et al. 2016).

Over the years, multispectral sensors with medium spatial resolution (10–30 m), such as: Landsat missions (MSS, TM, ETM+) (Sultan et al. 1987; Bennet et al. 1993; Elrakaiby 1995), ASTER (Rockwell and Hofstra 2008; Madani and Emam 2011; Mars and Rowan 2006; Mars and Rowan 2010) and SPOT (Bilotti et al. 2000; Kavak and Inan 2002; Ahmadirouhani and Samiee 2014), were the most frequently and widely used in geology. It is also worth mentioning that the European Space Agency (ESA) established the Copernicus European Earth Observation program to address issues related to the monitoring of the environment (Berger et al. 2012). Although Copernicus is not strictly geologically oriented, one of its missions, Sentinel-2, has proved to be sufficient for such analyses (van der Meer et al. 2012; van der Werff and van der Meer 2015).

Landsat Thematic Mapper images have been used especially for lithology mapping, the detection of lineaments, and to identify alteration mineralogy (van der Meer et al. 2012). We can, in particular, distinguish image analysis techniques such as: band rationing, decorrelation stretching or principal component (PC) analysis (van der Meer et al. 2012; Loughlin 1991; Tangestani and Moore 2002). Mineral exploration using remote-sensed data was also described in an article by Sabins (Sabins 1999), in which, based on data from Landsat TM, two assemblages of hydrothermal alteration minerals, iron minerals, and clays plus alunite were identified. Subsequently, based on hyperspectral data, individual types of iron and clay minerals were identified, which can provide details about hydrothermal zoning. Rockwell (Rockwell 2012, 2013) introduced a new methodology for the automated analysis of Landsat TM data that was applied to more than 180 images covering the western United States. This methodology was designed primarily for the regional mapping and characterization of exposed surface mineralogy, including that related to hydrothermal alteration and supergene weathering of pyritic rocks.

In the context of the presented research, it is worth mentioning papers that deal with mineral exploration. An interesting approach was demonstrated by the authors of the paper (Kereszturi et al. 2018), in which common classification algorithms (Random Forest) were trained using ground class data to identify volcanic terrains associated with hydrothermal alteration zones. Recognizing hydrothermally altered rocks through a combination of field data, mineralogical studies, spectral analysis as well as remote sensing techniques has been also shown in the work (Yousefi et al. 2018).

A similar approach was also presented by (Pournamdari and Hashim 2014), who demonstrated that the combination of ASTER and Landsat ETM data provides sufficient information to detect serpentinized dunites. Regarding the integration of remote sensing techniques and the classic geological approach, the authors of this article claim that remote sensing

methods are sensitive enough for exploration geologists and mining engineers to identify high-potential mineral zones, thus minimizing costly and time-consuming field works. An approach concerning the combination of ASTER and Landsat satellites was also shown in the paper (Safari et al. 2018): hydrothermally altered rocks associated with porphyry copper mineralization were identified using several band combinations, ratios and multiplications for both Landsat 8 and ASTER spectral bands.

Rajendran (Rajendran et al. 2012) also showed that satellites with medium spectral and spatial resolution are suitable for identifying serpentized harzburgites. Moreover, the quoted article also reflects contemporary exploration methods by which geologists, industrialists and mine owners are advised to adopt remote sensing techniques and avoid using only limited historical data for exploration and exploitation. Shalaby (Shalaby et al. 2010) showed how to combine classical geological methods with remote sensing. This kind of combination made it possible to define common characteristic features that led to the recognition of uranium mineralizations within the Pan-African younger granites of the Eastern Desert of Egypt. The above articles indicate that remote sensing techniques should be the standard for exploration geology. What is more, according to the paper (Pour et al. 2018), remote sensing techniques are especially useful when extreme environmental conditions inhibit direct surveying. The methodology presented in these works partly overlaps with the approach presented by the authors of this article. However, in contrast to the Middle East, Kosovo is often covered with dense green vegetation, which hinders the effectiveness of remote sensing techniques.

In the presented article, we introduce a comprehensive exploration method consisting of a series of activities to obtain the location of rocks similar to the measured sample, analyze results, and use geological maps for validation: acquisition of field samples, VNIR spectroscopy measurements that deal with the spectral curves of field samples, spectral image preprocessing, and the calculation of similarity coefficients.

Following the introduction, Section 2 addresses the research area and geology of the region. The authors' thesis and methodology are presented in Section 3. The data collection stage is presented in Section 4. Section 5 contains a description of the applied method for mineral prospecting based on the similarity between pixels and spectral curves. Section 6 deals with some practical examples and results. Also, the experimental evidence for the proposed solutions using field reconnaissance and a geology maps is shown in this section along with a discussion of the results. Finally, selected conclusions are summarized in Section 7.

## 1. Geology of the area of interest

The area of Selac lies in the Trepça Mineral Belt, not far from the famous Stan Terg deposit, the largest Pb-Zn deposit in Kosovo. The hydrothermal mineralization and alterations are related to the Tertiary (Oligocene-Miocene) volcanic activity that took place within the Trepça Mineral Belt, which is a part of the Vardar suture zone that stretches from the

north to the South through the Balkan Peninsula (Hyseni et al. 2010). The significance of the Trepça Mineral Belt has been confirmed by many authors who have described different types of Pb-Zn mineralization such as: skarn, hydrothermal replacement, disseminated, and vein, all of which are thought to be controlled primarily by faults.

The composition of the area in the broad surroundings of the Stan Terg deposit is as follows: Triassic sedimentary and volcanoclastic rocks; Upper Triassic carbonates; ophiolite

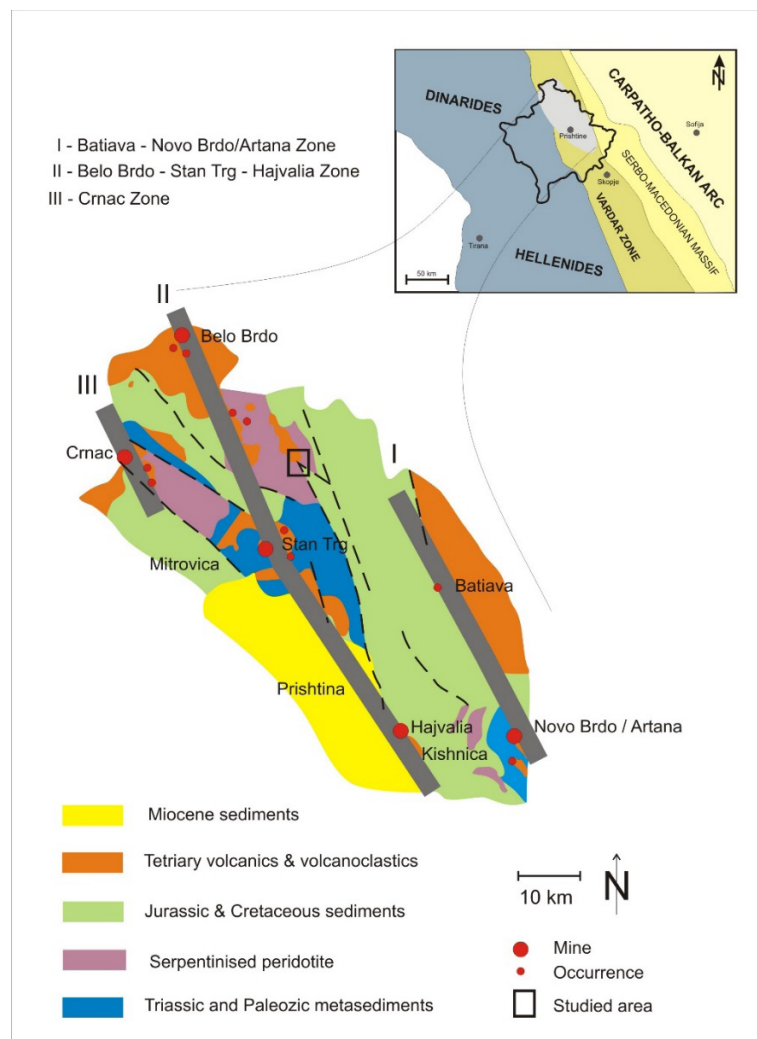


Fig. 1. Sample collection area; geotectonic setting of Vardar Zone and Trepça Mineral Belt units (Hyseni et al. 2010, modified). Three grey stripes represent mineralized zones (I, II, III). The zoom map in the upper right corner shows Kosovo's borders superimposed on the Trepça Mineral belt

Rys. 1. Obszar poboru próbek; sytuacja geotektoniczna strefy Vadar oraz pasa mineralnego Trepçy. Trzy szare pasy przedstawiają strefy zmineralizowane (I, II, III). Mapa w prawym górnym rogu przedstawia granice Kosowa naniesione na pas mineralny Trepçy

mélange with Jurassic ultrabasic rocks and serpentinites, and deep water metasediments; Cretaceous series of metasedimentary rocks; serpentinites, volcanics and volcanoclastic rocks of basaltic composition (diabases), carbonates. Tertiary volcanics and volcanoclastics (Fig. 1). The investigated area is covered mainly by serpentinites, ultramafic rocks, diabases, metasedimentary rocks of Triassic age, Tertiary volcanics such as lavas, and sub-volcanic intrusives and pyroclastic rocks that are dominated by trachyte, andesite and latite. Listvenite-like rocks occur on the borders between volcanic rocks and serpentinites, as well as in tectonic zones (silicified and carbonatized ultramafic rocks). These listvenites are usually mineralized, and gossan-like rocks occur in the weathered parts. The mineralization in the Stan Terg area is related to post-collisional magmatism (Palinkaš et al. 2013), and the nearest magmatic rocks of calc-alkaline composition that are exposed on the surface are in the Kopaonic Massif in northern Kosovo.

## 2. Methodology

This section describes all the steps of the method which was used for exploration of the area in question in Kosovo in detail. It should be mentioned that the authors' approach does not include drilling or geophysical research, which makes it fast, easy to interpret and low-cost. Therefore, depending on the type of exploratory research, the presented algorithm also optimizes the costs of drilling/geophysics by determining prospective areas and limiting the amount of work to be done.

The general outline of the procedure is described below in order to develop its individual steps in subsequent parts of the article:

- ◆ The first step is to analyze available geological materials and maps. Based on the collected data, a fragment of which is shown in Figure 1, the area of interest was indicated. Field research is the next step in our approach. Field teams collect rock material samples for further analysis. In addition, the GPS coordinates of each sample and a photograph of the relevant outcrop are obtained.
- ◆ Another element of the research is spectroscopic measurements of collected samples. The spectral characteristics and mineral composition of the samples are added to their geographical coordinates.
- ◆ The next step involves obtaining a collection of satellite images that cover the area defined in the first step. Subsequently, spectral characteristics are the input data for the developed algorithm that determines the similarity between the sample and the multispectral satellite imagery pixel. In addition, a green mask (based on the green vegetation index) is applied to increase the credibility of the final results, rejecting green areas that may affect the final results.

The final product is a map representing an image of the similarity between the rock sample and the satellite image. The results allow the area of interest to be narrowed. All the depicted areas were approved by field geologists as areas with a high chance of containing

the minerals that the authors were interested in. The final product was then used to develop more detailed geological research.

### 3. Data collection

This chapter describes the types of data and the way in which the authors acquired them. The first sub-chapter deals with satellite images, the second presents field studies and rock samples, while the third describes the measurements with a VNIR spectrometer.

#### 3.1. Satellite imagery

To provide efficient results, we first have to choose an appropriate image, i.e. one with minimal cloud, haze, dust, smoke, snow cover and maximal solar illumination (high solar elevation angle during late spring to early autumn) (Rockwell 2013). Therefore, considering the specificity of the area in question and the above requirements, we chose a Landsat 8 OLI LIT image from April 28 2013. The authors decided to choose Landsat 8 images for a few reasons, the most important of which was the availability of images for the region of Kosovo that would meet the requirements for the right season and the lack of cloud cover. Landsat provides images with 12-bit radiometric quantization and 190 km swath width. Scene metadata includes solar azimuth = 146, solar elevation = 57, and cloud cover = 1.40%. The scene was first radiometrically processed using Semi-Automatic Classification (Congedo 2016) to convert pixel DN values (i.e. Digital Numbers) to the physical measure of Top of Atmosphere reflectance (ToA) by applying the supplied gain and offset values. Finally, we obtain Surface Reflectance images using simple atmospheric correction DOS1 (Dark Object Subtraction 1), which is an image-based technique (Congedo 2016; Chavez 1996).

#### 3.2. Field data collection

The research area shown in Figure 2 was established based on geological maps and the true-color band compositions of acquired images, as well as exploration licenses.

During fieldwork, samples of various rock types were collected, including greenish or brown weathered soils, gossans, limestone stains, serpentinites, soil, sericite schists, diabase, and rock (dunites, serpentinites) in which chromites were visible. Four samples were selected (Table 1) as those representing rocks which were of interest to the authors. Samples were collected in order to represent the maximum outcrop exposure, as well as rocks and minerals that are characteristic of the area of interest. Sample photos of the field data collection areas are shown in Figure 3. Each sample was also localized by a GPS measurement. Moreover, areas showing the extent of gossan and diabase outcrops were determined during

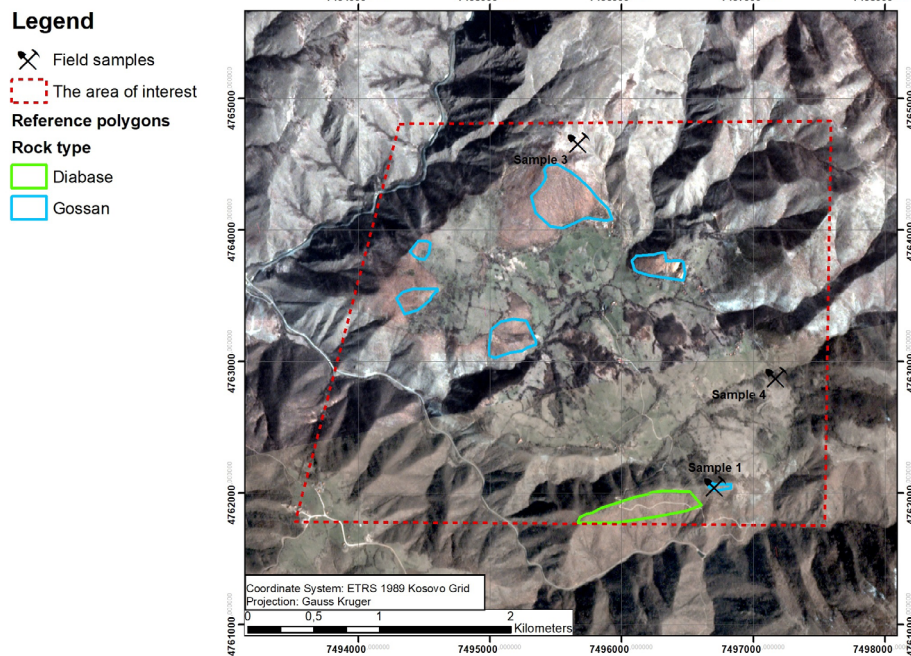


Fig. 2 The area of interest shown in true-color band compositions of high-resolution (3 meters) imagery delivered by Planet Lab, sensed on March 22, 2019

Rys. 2. Obszar badań przedstawiony w kolorach naturalnych przy użyciu kompozycji barwnej z wykorzystaniem zobrazowania wysokorozdzielczego (3 m) dostarczonego przez Planet Lab (zobrazowanie pozyskane przez satelitę 22 marca 2019)



Fig. 3. Collection of field sample (sample 2) – alteration zones visible

Rys. 3. Pobór próbki terenowej (próbka nr 2) – widoczne strefy alteracji

the fieldwork. Areas indicated during the fieldwork were used to assess a reliability of the results from remote sensing data.

Descriptions of the samples and the locations of their collection are shown below (Table 1).

Table 1. Description of the conditions in which the samples were collected

Tabela 1. Warunki poboru próbek

Sample ID	Description	Remarks
1	Gossan type outcrop	rock, dry sample
2	Greenish eluvium material	moist sample
3	Serpentine eluvium material, brown-green	moist sample
4	Altered diabase, greenschist	moist sample

### 3.3. Spectroscopy measurements

Spectroscopic measurements were performed on the collected rock samples to determine their spectral signatures. The measurements were taken using a Terraspec HALO spectrometer, which is intended for geological measurements. The spectrometer measures the full visible range and infrared wavelengths (350–2500 nm). The imaging resolution is 3 nm @ 700 nm, 8.3 nm @ 1400 and 9.6 @ 2150 nm. The measured spectral signatures are also compared with the USGS spectral curves, which allows the mineral composition of the sample and the level of confidence to be estimated (Table 2).

Table 2. The mineral composition of samples obtained during spectroscopy measurements

Tabela 2. Skład mineralny poszczególnych próbek uzyskany podczas pomiarów spektrometrem

Sample ID	Mineral composition
1	Chabazite 3, Iron Saponite 3, Goethite 3
2	Goethite 3, Gmelinite-Na 3, Hectorite 3, Nontronite 2
3	Goethite 3, Iron Smectite 3, Hectorite 3, Gypsum 3
4	Goethite 2, Iron Smectite 3, Magnesite 3

Number next to mineral indicates confidence: 3 – 90% confidence; 2 – 60–90% confidence; 1 – less than 60% confidence.

The measurements were performed in the laboratory, on a flat surface if possible, by applying the spectrometer to the upper surface of the sample. Several measurements were taken for each sample. Each single measurement of the sample also had a unique identifier; this facilitated the further interpretation of the data. The results are shown in Figure 4.



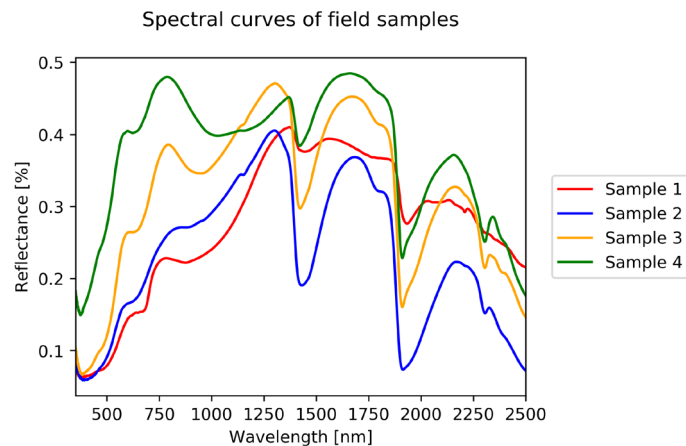


Fig. 4. Plots for spectral curves of four samples

Rys. 4. Krzywe spektralne dla wszystkich czterech próbek

The next step was to convert the sample measurement DN to Surface Reflectance using the spectrometer's built-in software. In addition to the spectral signature, the spectrometer also identifies the mineral composition of the sample, as shown in Table 2. Identified minerals should be analyzed with reference to the number next to the name of each mineral. Number 3 indicates 96% certainty of measurement; 2 indicates 80% certainty; 1 indicates an uncertain measurement of less than 40% certainty.

#### 4. Methods of data comparison

This chapter describes the authors' method of determining the similarity coefficient between each rock sample and the satellite image used for experiments.

The method uses rock samples collected in-situ for the desired type of rock or mineral. This allows for a comparison of the reflectance of rock samples against the surface reflectance obtained from satellite images. If the reflectance obtained in some pixel is similar to the reflectance of a rock sample, we classify it as a place where the related type of rock can be found.

The method used in our article is customized to a small amount of reference data. The method involves seeking pixels in the satellite image that best match the reference spectrum, which is measured on rock samples in the laboratory. It compares only angles between vectors in N-dimensional space and is independent of the length of either vector. This property is useful when the data is not corrected for topographic shading (Schowengerdt 2006). As a result, areas that consist of pixels with reflectance equal to the reflectance of rock samples gathered in the field are obtained.

To classify the pixels in the satellite images we used the spectral curves recorded by a Terraspec HALO spectrometer on rock samples gathered in the field. The measured reflectance is then averaged in seven bands that match the seven bands of the OLI camera (Fig. 5). Band eight is excluded because it overlaps with band 2 (partly), 3 and 4. Band 9 is excluded because it provides information from clouds rather than from the earth's surface. Bands 10 and 11 are also excluded because they are far beyond the range of the spectrometer.

For each pixel of the investigated area, the similarity coefficient  $\text{sim}(k)$  is evaluated. This makes it possible to compare the averaged reflectance in selected spectral bands to the reflectance of the OLI camera using the angular distance between two  $N$ -dimensional vectors (in our case  $N = 7$ ):

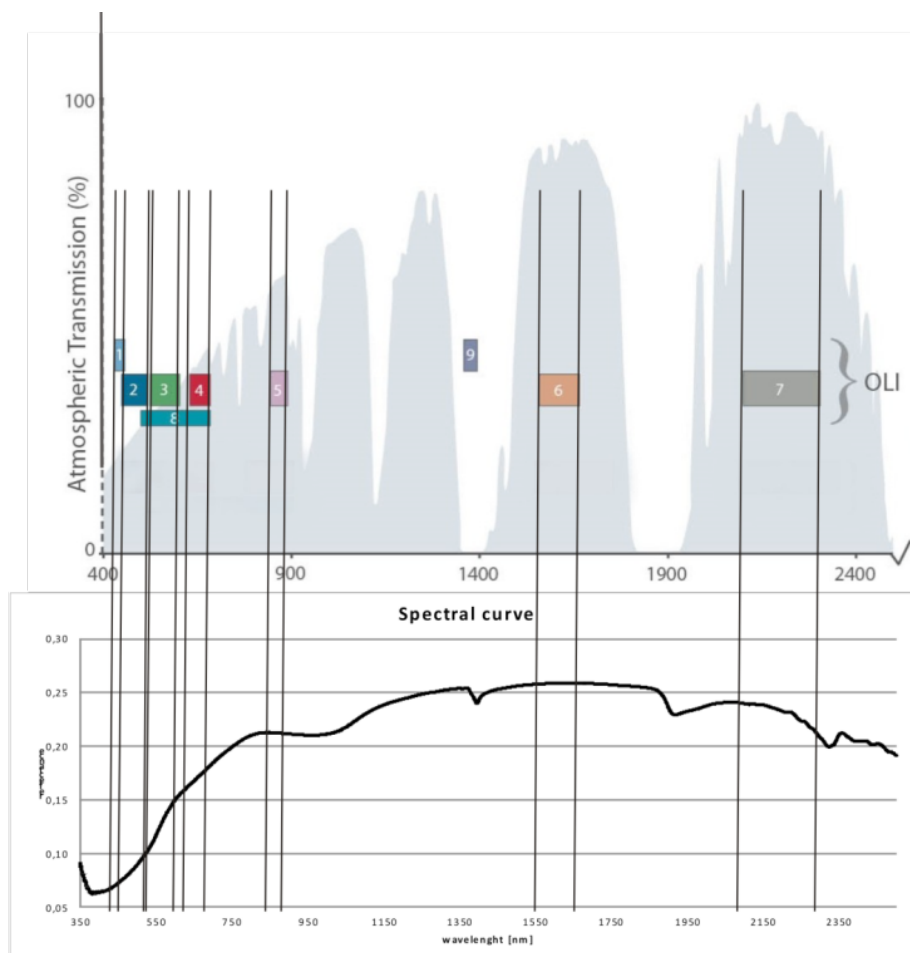


Fig. 5. An example of averaging a field sample in specific Landsat 8 bands

Rys. 5. Przykład uśredniania pomiarów dla próbek terenowych dla określonych kanałów satelity Landsat 8

$$sim(k) = a \cos \left( \frac{\sum_{i=1}^7 (hip_i \times ol_i)}{\sqrt{\sum_{i=1}^7 (hip_i)^2} \sqrt{\sum_{i=1}^7 (ol_i)^2}} \right)$$

- $i$  – band number  $i = 1, \dots, 7$ ,  
 $hip_i$  – averaged reflectance measured over the rock sample in band  $i$ ,  
 $ol_i$  – reflectance for an analyzed pixel in band  $i$ ,  
 $k$  – number of field sample  $k = 1, \dots, 19$ .

The similarity coefficient was evaluated for every measured spectrum and for spectra averaged for the given rock sample. The smallest values of the similarity coefficient are related to the highest similarity of the given rock sample's reflectance to the reflectance obtained from the OLI image.

The similarity coefficients were then sorted in ascending order, therefore the best-fitting spectra were grouped at the beginning of the sorted series. To choose the most significant values, the entire range of similarity values was divided into 20 classes according to 20 quantiles. The pixels with the lowest 5% of similarity coefficients were regarded as places where minerals occur. This makes it possible to map the possible locations of every examined sample.

The method of classification proposed here is most effective if the investigated area is comparable to the resolution of the OLI camera in the used bands (e.g. 30 m). The proposed classification method is also effective if the rocks/minerals in the investigated area were created in similar conditions. This makes it possible to expect spectral similarities of samples of the same kind of rock or mineral.

## 5. Results

The research results were verified by observations made by geologists during the field-work. Areas where outcrops of particular rocks were observed are marked on the following maps as Reference polygons.

For every sample, the range marked with diagonal lines represents the first quantile of the coefficient of similarity between the satellite image and the sample. For all samples, a background geological map was used to show the basic geological features in the field. As presented, the northern part of the investigation area and partly the western and southern areas are made of listvenite-type rocks (hydrothermally altered serpentinites with gossans); the central part is made of volcanic-volcano sedimentary complexes; diabases occur in the southern and partly in the south-eastern part.

The main areas where similarity was detected were a big alteration zone with gossan in the northern part of the map (Islaimovici), and another in the western part, where a similar gossan type of material is common. The southern part is formed on basalts, where outcrops of rock units are strongly weathered; moreover, serpentinites are also exposed in some small parts of the ridge area. Due to this, part of this region was also highlighted by similarity computations.

In the central part, which is made of volcanic rocks, there are no similarities with any sample of the gossan type of material because of the extensive soil coverage.

As can be observed in Figures 6–9, for all samples the highest similarity between the rock sample and the satellite image occurs in almost the same places, with small differences. This sort of result was expected. Even so, samples were collected from different rock units and were determined to have a varying mineral composition; all represent weathered material of the same type that can be observed in most of the areas in question. The results are also compatible with the designated reference polygons.

The proposed technique of determining the degree of similarity between a rock sample and a given pixel works efficiently.

Assessing the obtained results, we can conclude that the discussed remote sensing techniques can be considered useful for mineral prospecting, especially in less accessible areas.

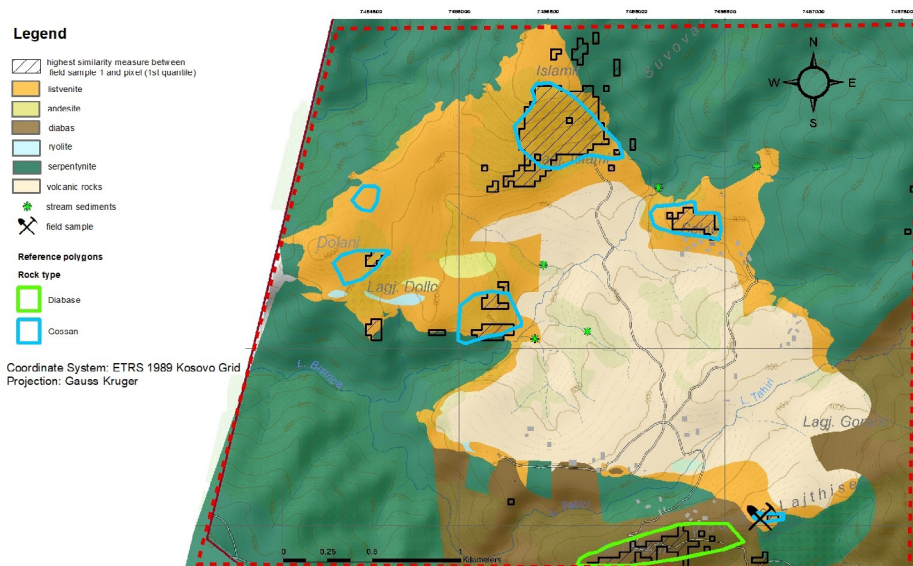


Fig. 6. Comparison of the similarity coefficient between rock sample 1 and the satellite image. The geological map used as a background

Rys. 6. Porównanie współczynnika podobieństwa pomiędzy próbką 1 oraz zobrażeniem satelitarnym. W tle mapa geologiczna

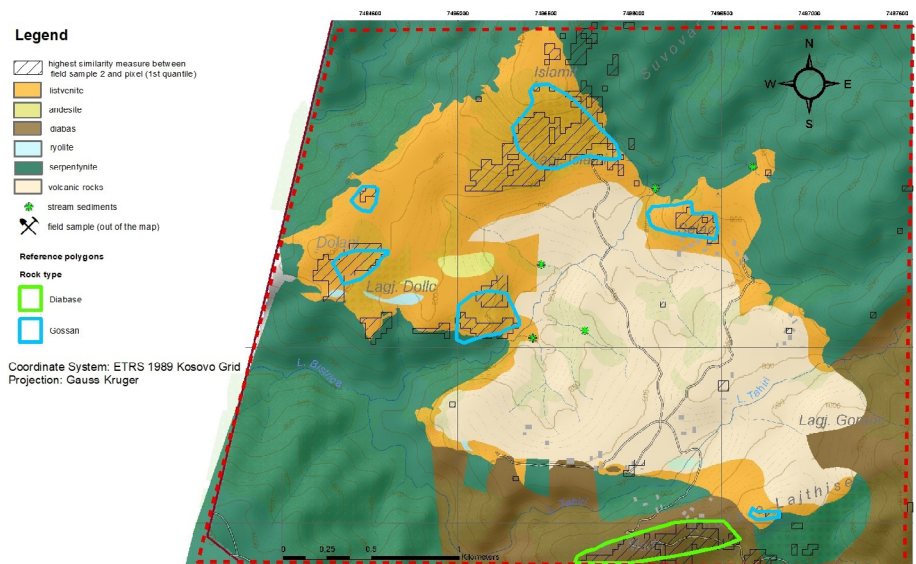


Fig. 7. Comparison of the similarity coefficient between rock sample 2 and the satellite image.  
The geological map used as a background

Rys. 7. Porównanie współczynnika podobieństwa pomiędzy próbką 2 oraz zobrazeniem satelitarnym.  
W tle mapa geologiczna

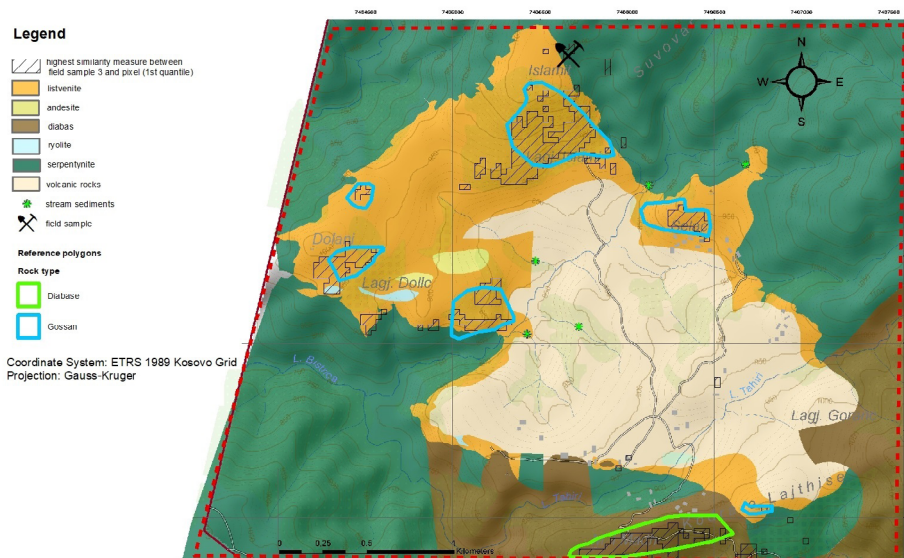


Fig. 8. Comparison of the similarity coefficient between rock sample 3 and the satellite image.  
The geological map used as a background

Rys. 8. Porównanie współczynnika podobieństwa pomiędzy próbką 3 oraz zobrazeniem satelitarnym.  
W tle mapa geologiczna

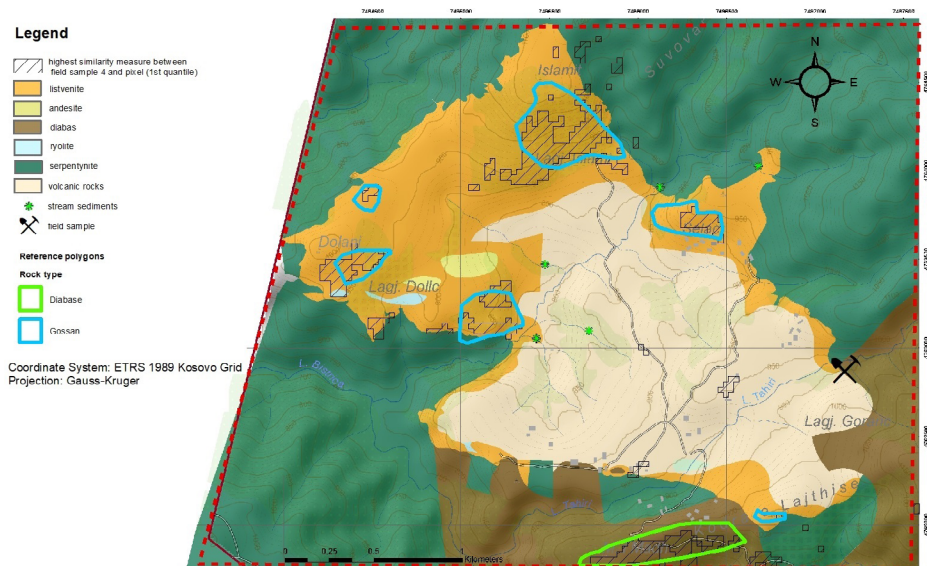


Fig. 9. Comparison of the similarity coefficient between rock sample 4 and the satellite image. The geological map used as a background

Rys. 9. Porównanie współczynnika podobieństwa pomiędzy próbką 4 oraz zobrażeniem satelitarnym. W tle mapa geologiczna

Properly processed satellite images are intended to determine zones of mineralization and alteration as well as the distribution of individual minerals, without the need to visit a given area. The main advantage of this approach is the possibility of reducing the cost of prospecting by determining potential areas of interest. However, the effectiveness of remote sensing methods could be increased by combining imagery products with classic detailed mineralogical investigations such as: XRD, XRF, LA ICP-MS, Raman spectroscopy and classical microscopy. For this approach, after the first remote sensing investigation and the first field reconnaissance, a mineralogical examination and validation of the similarity indices/coefficients could be performed. Subsequently, re-calculated similarity measures for individual minerals could then be used for areas with equal geology. Increasing the accuracy of the described approach also depends on the quality of data. Therefore, the use of high-resolution airborne hyperspectral imagery is likely to enable such studies even in wooded areas due to better resolution, both spectral and spatial.

## Conclusions

In this article, we introduced a remote sensing technique to identify mineral prospective areas. Sections 3–5 contain a detailed description of the methodology that was adopted by

the authors of this article. For the purposes of this research, four rock samples were analyzed. First, their spectral characteristics were measured in the laboratory; subsequently, the proposed method was used to measure the similarity between each sample and the respective multispectral satellite images. Section 6 contains an interpretation of the results based on the collected data and the geological map that was prepared by the authors of this article.

It was shown that the free multispectral data obtained by the Landsat 8 satellite, even with average resolution, can be considered a valuable source of information that helps narrow down the exploration areas. This approach can help reduce the cost of geological works, thereby making mineral prospecting profitable in difficult-to-access areas. However, the reliability of the results of the described method depends largely on the quality of the satellite imagery used. Due to the fact that there are no hyperspectral satellite imagery available at present, the only source of data with satisfactory spatial and spectral resolution is airborne imagery. However, the cost of acquiring this sort of data is high, which runs counter to the original aim of this article, which was to focus on low-cost methods. Nevertheless, combining the described technology with the use of airborne imagery will be the subject of further research conducted by the authors of this article.

*Author Contributions: Michał Lupa put forward the original idea, designed the methodology, performed the examples and drafted the manuscript. Andrzej Leśniak designed the methodology, analyzed the data and revised the manuscript. Jaroslav Pršek conducted and described the geological analysis. Katarzyna Adamek created and interpreted the result maps.*

*The work is partially financed by the Faculty of Geology, Geophysics and Environmental Solutions, AGH University of Science and Technology in Kraków.*

## REFERENCES

- Ahmadirouhani, R. and Samiee, S. 2014. Mapping glauconite unites with using remote sensing techniques in north east of Iran. *1<sup>st</sup> Isprs International Conference on Geospatial Information Research* 40, pp. 7–11.
- Bedini, E., van der Meer, F. and van Ruitenbeek, F. 2009. Use of HyMap imaging spectrometer data to map mineralogy in the Rodalquilar caldera, southeast Spain. *International Journal of Remote Sensing* 30, pp. 327–348.
- Berger et al. 2012 – Berger, M., Moreno, J., Johannessen, J.A., Levelt, P.F. and Hanssen, R.F. 2012. ESA's sentinel missions in support of Earth system science. *Remote Sensing of Environment* 120, pp. 84–90.
- Bielecka et al. 2014 – Bielecka, M., Porzycka-Strzelczyk, S. and Strzelczyk, J. 2014. SAR images analysis based on polarimetric signatures. *Applied Soft Computing* 23, pp. 259–269.
- Bilotti et al. 2000 – Bilotti, F., Shaw, J.H. and Brennan, P. A. 2000. Quantitative structural analysis with stereoscopic remote sensing imagery. *AAPG Bulletin* 84, pp. 727–740.
- Chavez, P.S. 1996. Image-based atmospheric corrections-revisited and improved. *Photogrammetric engineering and remote sensing* 62, pp. 1025–1035.
- Cloutis, E.A. 1996. Review article hyperspectral geological remote sensing: evaluation of analytical techniques. *International Journal of Remote Sensing* 17, pp. 2215–2242.
- Congedo, L. 2016. Semi-automatic classification plugin documentation. Release, 4, p. 29.
- Dasgupta, S. and Mukherjee, S. 2019. *Remote sensing in lineament identification: examples from western India. Developments in Structural Geology and Tectonics*. Elsevier.

- Elrakaiby, M. L. 1995. The use of enhanced landsat-tm image in the characterization of uraniferous granitic-rocks in the central eastern desert of Egypt. *International Journal of Remote Sensing* 16, pp. 1063–1074.
- Fraser et al. 1997 – Fraser, A., Huggins, P., Rees, J. and Cleverly, P. 1997. A satellite remote sensing technique for geological structure horizon mapping. *International Journal of Remote Sensing* 18, pp. 1607–1615.
- Goetz et al. 1985 – Goetz, A.F.H., Vane, G., Solomon, J.E. and Rock, B.N. 1985. Imaging spectrometry for earth remote-sensing. *Science* 228, pp. 1147–1153.
- Hyseni et al. 2010 – Hyseni, S., Durmishaj, B., Fetahaj, B., Shala, F., Berisha, A. and Large, D. 2010. Trepça Ore Belt and Stan Terg mine-Geological overview and interpretation, Kosovo (SE Europe). *Geologija* 53, pp. 87–92.
- Joyce et al. 2014 – Joyce, K.E., Samsonov, S.V., Levick, S.R., Engelbrecht, J. and Belliss, S. 2014. Mapping and monitoring geological hazards using optical, LiDAR, and synthetic aperture RADAR image data. *Natural Hazards* 73, pp. 137–163.
- Kavak, K. and Inan, S. 2002. Enhancement facilities of SPOT XS imagery in remote sensing geology: an example from the Sivas Tertiary Basin (central Anatolia/Turkey). *International Journal of Remote Sensing* 23, pp. 701–710.
- Kereszturi et al. 2018 – Kereszturi, G., Pullanagari, R., Mead, S., Schaefer, L., Procter, J., Schleiffarth, W. and Kennedy, B. 2018. Geological Mapping of Hydrothermal Alteration on Volcanoes from Multi-Sensor Platforms. IGARSS 2018–2018 IEEE International Geoscience and Remote Sensing Symposium, 2018. IEEE, pp. 220–223.
- Loughlin, W.P. 1991. Principal component analysis for alteration mapping. *Photogrammetric Engineering and Remote Sensing* 57, pp. 1163–1169.
- Madani, A. and Emam, A. 2011. SWIR ASTER band ratios for lithological mapping and mineral exploration: a case study from El Hudi area, southeastern desert, Egypt. *Arabian Journal of Geosciences* 4, pp. 45–52.
- Mars, J.C. and Rowan, L.C. 2006. Regional mapping of phyllic-and argillic-altered rocks in the Zagros magmatic arc, Iran, using Advanced Spaceborne Thermal Emission and Reflection Radiometer (ASTER) data and logical operator algorithms. *Geosphere* 2, pp. 161–186.
- Mars, J.C. and Rowan, L.C. 2010. Spectral assessment of new ASTER SWIR surface reflectance data products for spectroscopic mapping of rocks and minerals. *Remote Sensing of Environment* 114, pp. 2011–2025.
- Mierczyk et al. 2016 – Mierczyk, M., Zagajewski, B., Jarocinska, A. and Knapik, R. 2016. Assessment of Imaging Spectroscopy for rock identification in the Karkonosze Mountains, Poland. *Miscellanea Geographica* 20, pp. 34–40.
- Palinkaš et al. 2013 – Palinkaš, S.S., Palinkaš, L.A., Renac, C., Spangenberg, J.E., Lüders, V., Molnar, F. and Maliqi, G. 2013. Metallogenic model of the Trepča Pb-Zn-Ag skarn deposit, Kosovo: evidence from fluid inclusions, rare earth elements, and stable isotope data. *Economic Geology* 108, pp. 135–162.
- Porzycka, S. and Leśniak, A. 3D GIS analysis of PSInSAR data as a source of information in monitoring of areas endangered by terrain deformations.
- Pour et al. 2018 – Pour, A.B., Hashim, M., Park, Y. and Hong, J.K. 2018. Mapping alteration mineral zones and lithological units in Antarctic regions using spectral bands of ASTER remote sensing data. *Geocarto International* 33, pp. 1281–1306.
- Pournamdari, M. and Hashim, M. 2014. Detection of chromite bearing mineralized zones in Abdasht ophiolite complex using ASTER and ETM+ remote sensing data. *Arabian Journal of Geosciences* 7, pp. 1973–1983.
- Rajendran et al. 2012 – Rajendran, S., Al-Khribash, S., Pracejus, B., Nasir, S., Al-Abri, A.H., Kusky, T.M. and Ghulam, A. 2012. ASTER detection of chromite bearing mineralized zones in Semail Ophiolite Massifs of the northern Oman Mountains: Exploration strategy. *Ore geology reviews* 44, pp. 121–135.
- Rockwell, B.W. 2012. Description and validation of an automated methodology for mapping mineralogy, vegetation, and hydrothermal alteration type from ASTER satellite imagery with examples from the San Juan Mountains, Colorado. US Geological Survey.
- Rockwell, B.W. 2013. Automated mapping of mineral groups and green vegetation from Landsat Thematic Mapper imagery with an example from the San Juan Mountains, Colorado. US Geological Survey Scientific Investigations Map, 3252.
- Rockwell, B.W. and Hofstra, A.H. 2008. Identification of quartz and carbonate minerals across northern Nevada using ASTER thermal infrared emissivity data-Implications for geologic mapping and mineral resource investigations in well-studied and frontier areas. *Geosphere* 4, pp. 992–992.



- Bennet et al. 1993 – Bennet, S.A., Atkinson Jr, W.W. and Kruse, F.A. 1993. Use of Thematic Mapper Imagery to Identify Mineralization in the Santa Teresa District, Sonora, Mexico. *International Geology Review*.
- Sabins, F.F. 1999. Remote sensing for mineral exploration. *Ore Geology Reviews* 14, pp. 157–183.
- Safari et al. 2018 – Safari, M., Maghsoudi, A. and Pour, A.B. 2018. Application of Landsat-8 and ASTER satellite remote sensing data for porphyry copper exploration: a case study from Shahr-e-Babak, Kerman, south of Iran. *Geocarto international* 33, pp. 1186–1201.
- Schowengerdt, R.A. 2006. Remote sensing: models and methods for image processing, Elsevier.
- Shalaby et al. 2010 – Shalaby, M., Bishra, A. and Roz, M. 2010. Integration of geologic and remote sensing studies for the discovery of uranium mineralization in some granite plutons, Eastern Desert, Egypt. *Journal of King Abdulaziz University: Earth Sciences* 150, pp. 1–50.
- Sultan et al. 1987 – Sultan, M., Arvidson, R.E., Sturchio, N.C. and Guinness, E.A. 1987. Lithologic mapping in arid regions with landsat thematic mapper data - meatiq dome, Egypt. *Geological Society of America Bulletin* 99, pp. 748–762.
- Tangestani, M.H. and Moore, F. 2002. Porphyry copper alteration mapping at the Meiduk area, Iran. *International Journal of Remote Sensing* 23, pp. 4815–4825.
- van der Meer et al. 2012 – van der Meer, F.D., van der Werff, H.M.A., Van Ruitenbeek, F.J.A., Hecker, C.A., Bakker, W.H., Noomen, M.F., van der Meijde, M., Carranza, E.J.M., de Smeth, J.B. and Woldai, T. 2012. Multi- and hyperspectral geologic remote sensing: A review. *International Journal of Applied Earth Observation and Geoinformation* 14, pp. 112–128.
- van der Werff, H. and van der Meer, F. 2015. Sentinel-2 for mapping iron absorption feature parameters. *Remote sensing* 7, pp. 12635–12653.
- Yousefi et al. 2018 – Yousefi, S.J., Ranjbar, H., Alirezaei, S., Dargahi, S. and Lentz, D.R. 2018. Comparison of hydrothermal alteration patterns associated with porphyry Cu deposits hosted by granitoids and intermediate-mafic volcanic rocks, Kerman Magmatic Arc, Iran: Application of geological, mineralogical and remote sensing data. *Journal of African Earth Sciences* 142, pp. 112–123.
- Zagajewski, B., Tommervik, H., Bjerke, J., Raczko, E., Bochenek, Z., Kłos, A., Jarocińska, A., Lavender, S. and Ziółkowski, D. 2017. Intraspecific differences in spectral reflectance curves as indicators of reduced vitality in high-arctic plants. *Remote Sensing* 9, p. 1289.

#### APPLICATION OF SATELLITE REMOTE SENSING METHODS IN MINERAL PROSPECTING IN KOSOVO, AREA OF SELAC

#### Keywords

remote sensing, GIS, geology, mineral mapping, Landsat 8

#### Abstract

Traditional methods of mineral exploration are mainly based on very expensive drilling and seismic methods. The proposed approach assumes the preliminary recognition of prospecting areas using satellite remote sensing methods. Maps of mineral groups created using Landsat 8 images can narrow the search area, thereby reducing the costs of geological exploration during mineral prospecting. This study focuses on the identification of mineralized zones located in the southeastern part of Europe (Kosovo, area of Selac) where hydrothermal mineralization and alterations can be found. The article describes all the stages of research, from collecting in-situ rock samples, obtaining spectral characteristics with laboratory measurements, preprocessing and analysis of satellite images, to the validation of results through field reconnaissance in detail. The authors introduce a curve-index fitting

technique to determine the degree of similarity of a rock sample to a given pixel of satellite imagery. A comparison of the reflectance of rock samples against surface reflectance obtained from satellite images allows the places where the related type of rock can be found to be determined. Finally, the results were compared with geological and mineral maps to confirm the effectiveness of the method. It was shown that the free multispectral data obtained by the Landsat 8 satellite, even with a resolution of 30 meters, can be considered as a valuable source of information that helps narrow down the exploration areas.

#### WYKORZYSTANIE METOD TELEDETEKCYJ SATELITARNEJ W POSZUKIWANIU ZŁÓŻ SUROWCÓW MINERALNYCH W REJONIE SELAC, KOSOWO

##### Słowa kluczowe

GIS, teledetekcja, geologia, Landsat 8, geologiczne poszukiwania surowców mineralnych

##### Streszczenie

Tradycyjne metody poszukiwania surowców mineralnych opierają się głównie na bardzo kosztownych metodach, takich jak wiercenia oraz metody sejsmiczne. Proponowane przez autorów podejście zakłada wstępne rozpoznanie obszarów perspektywicznych z wykorzystaniem metod teledetekcji satelitarnej. Mapy grup minerałów stworzone przy użyciu zobrażeń dostarczonych przez satelitę Landsat 8 mogą zawęzić obszar poszukiwań, a przez to doprowadzić do redukcji kosztów rozpoznania geologicznego podczas poszukiwania surowców mineralnych. Niniejsze badanie skupia się na identyfikacji stref zmineralizowanych znajdujących się w południowo-wschodniej Europie (Kosowo, rejon Selac) gdzie znajdują się mineralizacje hydrotermalne oraz strefy alteracji. Artykuł opisuje szczegółowo wszystkie etapy badań, od pozyskania próbek terenowych, badań laboratoryjnych mających na celu pozyskanie charakterystyk spektralnych, przez wstępne przetwarzanie oraz analizę zobrażeń satelitarnych do walidacji wyników poprzez rozpoznanie terenowe. Autorzy przedstawili technikę wykorzystującą wskaźnik dopasowania krzywej pozwalający na określenie stopnia podobieństwa próbki do piksela zobrażenia satelitarnego. Porównanie współczynnika odbicia dla próbek względem współczynnika odbicia zarejestrowanego przez satelitę pozwala na określenie miejsc, gdzie mogą występować określone typy skał. W celu określenia skuteczności metody wyniki zostały porównane z mapami geologicznymi. Wykazano, że darmowe dane multispektralne dostarczone przez satelitę Landsat 8, nawet z rozdzielczością 30 m, mogą stanowić cenne źródło informacji, które pozwala na zawężenie obszaru poszukiwań.